



Palladium nanoparticles immobilized on sepiolite–cyclodextrin nanosponge hybrid: Efficient heterogeneous catalyst for ligand- and copper-free C–C coupling reactions

Samahe Sadjadi¹ | Majid M. Heravi² | Maryam Raja² | Fatemeh Ghoreyshi Kahangi³

¹ Gas Conversion Department, Faculty of Petrochemicals, Iran Polymer and Petrochemicals Institute, Tehran, Iran

² Department of Chemistry, School of Science, Alzahra University, Vanak, Tehran, Iran

³ Department of Chemistry, University of Gilan, Rasht, Iran

Correspondence

Samahe Sadjadi, Gas Conversion Department, Faculty of Petrochemicals, Iran Polymer and Petrochemicals Institute, PO Box 14975-112, Tehran, Iran.
Email: samahesadjadi@yahoo.com; s.sadjadi@ippi.ac.ir

Majid M. Heravi, Department of Chemistry, School of Science, Alzahra University, PO Box 1993891176, Vanak, Tehran, Iran.
Email: mmh1331@yahoo.com; m.heravi@alzahra.ac.ir

Funding information

Iran Polymer and Petrochemical Institute and Alzahra University; Iran National Science Foundation

A novel hybrid system composed of sepiolite clay and cyclodextrin nanosponge (CDNS) was prepared via reaction of Cl-functionalized sepiolite with amine-functionalized CDNS. CDNS–sepiolite was then applied for immobilization of Pd(0) nanoparticles. The resulting hybrid system, Pd@CDNS–sepiolite, was characterized using various techniques and successfully used as an efficient and heterogeneous catalyst for ligand- and copper-free Sonogashira and Heck coupling reactions under mild reaction conditions. Recycling experiments confirmed that Pd@CDNS–sepiolite was recyclable and could be used for several consecutive reaction runs with slight Pd leaching and loss of catalytic activity.

KEYWORDS

C–C coupling reactions, cyclodextrin nanosponge, Pd nanoparticles, sepiolite

1 | INTRODUCTION

Cyclodextrin nanosponges (CDNSs), three-dimensional polymeric network systems, are derived from the reaction of a cross-linker^[1,2] such as carbonyl diimidazole and diarylcarbonates^[3] with cyclodextrins (CDs) as monomers. The presence of CDs, which naturally have cavities, as well as the porous structure of a polymeric network render CDNSs promising candidates for accommodating diverse range of guest molecules with various sizes, shapes and polarities from drugs and organic compounds to catalytic active species.^[1,2,4,5] The high thermal and pH stability of CDNSs as well as biocompatibility expand their utility.^[1,6–10] Recently,

the applications of CDNSs in various research fields such as drug delivery^[11–13] and catalysis have been growing.^[1,14–18]

Sepiolite is a naturally occurring hydrated Mg–Al silicate fibrous clay with the general formula of Mg₈Si₁₂O₃₀(OH)₄(OH₂)₄·nH₂O (Figure S1 in supporting information).^[19] As sepiolite is an assembly of needle-like particles separated by parallel channels,^[20] it possesses an open porous framework. Each structural unite of sepiolite is composed of two tetrahedral silica sheets and a central octahedral sheet containing magnesium.^[21] The porous nature of sepiolite as well as its high surface area make it a suitable candidate for supporting various catalytic species and developing novel heterogeneous (photo)catalysts.^[22–24]

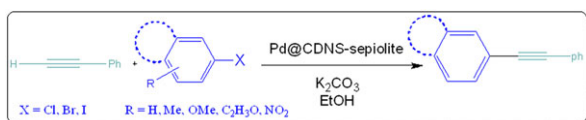
Among various organic transformations, C–C coupling reactions such as Heck and Sonogashira reactions are of great importance. These Pd-catalysed reactions are potent tools for the synthesis of natural products or complicated chemicals with biological activities.^[25] Classically, these coupling reactions proceed in the presence of phosphine ligands and copper co-catalysts.^[26,27] Development of copper- and ligand-free protocols^[28] with the use of heterogeneous catalysts in aqueous media is considered as a turning point in this field and can facilitate the applications of such processes for industrial purposes.^[26,29–40] As an example, immobilization of Pd on cellulose–aluminium oxide composite^[41] and biopolymers^[42–45] can be mentioned. In this context, use of biopolymers such as wool, chitosan and cellulose as catalyst supports has attracted much attention due to their biodegradability, biocompatibility, chemical and physical versatility, availability and relatively low cost. Notably, most biopolymers can be chemically modified or hybridized with other materials.^[42–45]

In the course of our research on heterogeneous catalysis,^[46–49] recently we reported the utility of CDNS and natural clays for immobilizing catalytic active species.^[50] In this line, it was found that the hybridization of inorganic supports with CDNS can lead to an improvement of the catalytic performance of the resulting catalyst.^[51] Considering this issue, herein we report the utility of a CDNS–sepiolite hybrid system for immobilization of Pd(0) nanoparticles and development of a heterogeneous catalyst, Pd@CDNS–sepiolite, with the utility of promoting Sonogashira and Heck reactions (Schemes 1 and 2). Furthermore, the recyclability of Pd@CDNS–sepiolite and Pd leaching upon recovery and recycling were investigated.

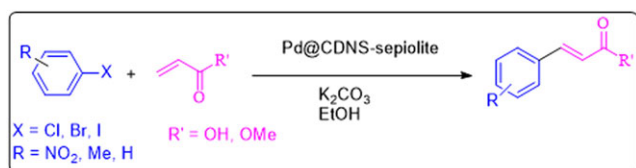
2 | EXPERIMENTAL

2.1 | Materials and Instrumentation

To prepare the catalyst, the following reagents were used: sepiolite clay, diphenyl carbonate, β -cyclodextrin, Pd



SCHEME 1 Sonogashira reaction.



SCHEME 2 Heck reaction.

(OAc)₂, NaBH₄, (3-chloropropyl) trimethoxysilane, N-[3-(trimethoxysilyl)propyl] ethylenediamine (AEAPTMS), toluene and MeOH. All were of analytical grade and purchased from Sigma-Aldrich and used without further purification. Sepiolite clay, PANGEL S9, was provided from TOLSA.

The organic reagents for performing Heck and Sonogashira coupling reactions included aryl halides, acetylenes, K₂CO₃, alkenes and EtOH. All were of analytical grade and purchased from Merck and used without further purification.

The structure of the hybrid catalyst was confirmed using various characterization techniques including X-ray diffraction (XRD), Fourier transform infrared (FT-IR) spectroscopy and thermogravimetric analysis (TGA). The morphology of the catalyst was studied by recording scanning electron microscopy (SEM)/energy-dispersive spectroscopy (EDS) and transmission electron microscopy (TEM) images. Moreover, the content of Pd nanoparticles in the catalyst was estimated using inductively coupled plasma atomic emission spectrometry (ICP-AES). The textural properties of the catalyst were investigated using Brunauer–Emmett–Teller measurements. SEM/EDS images of Pd@CDNS–sepiolite and its components were recorded with a Tescan instrument. A BELSORP Mini II apparatus was used for studying the textural properties of the catalyst. To degas the catalyst, it was heated at 423 K for 4 h. XRD patterns of sepiolite and Pd@CDNS–sepiolite were recorded using a Siemens D5000 with Cu K α radiation from a sealed tube. A Mettler Toledo TGA instrument was employed for accomplishing TGA, using nitrogen atmosphere and a heating rate of 10 °C min⁻¹ in the range 30–700 °C. FT-IR spectra were recorded with a PerkinElmer Spectrum 65 instrument. TEM analyses were performed using a Philips CM30300Kv field emission transmission electron microscope. To perform this analysis, the samples were coated with gold. To perform ICP analysis, an ICP analyser (Vista-pro, Varian) was employed.

Heck and Sonogashira coupling reactions were monitored using HPLC (Agilent-1100). As all the organic products of Heck and Sonogashira reactions were previously reported, their formation was validated by comparing their melting points, determined in open capillaries using an Electrothermal 9100 without further corrections, and FT-IR spectra with those of known samples. To further confirm the structure of the products, some selected products were characterized using ¹H NMR and ¹³C NMR spectroscopy, with a Bruker DRX-400 spectrometer at 400 and 100 MHz, respectively.

2.2 | Synthesis of CDNS

To prepare CDNS (1), the melting approach was applied.^[4,5,9] Briefly, cross-linking agent diphenyl carbonate (8 mmol) was melted. Then, β -cyclodextrin (1 mmol), which served as monomer, was added to the melted

cross-linking agent. The polymerization reaction proceeded by stirring the mixture at 120 °C for 12 h. At the end of the reaction, the obtained white solid was cooled to room temperature and milled. Subsequently, to purify CDNS and remove phenol by-product that formed in the course of the reaction, a solution NaOH was added to an aqueous suspension of CDNS and the resulting mixture was stirred for 5 h to let the phenol become soluble sodium phenoxide. Then, the CDNS was filtered off and repeatedly washed with acetone and distilled water. Further purification was performed by Soxhlet extraction with EtOH for 4 h. To ensure successful removal of phenol, the purified CDNS was suspended in basic aqueous medium and stirred for 3 h. Then, CDNS was filtered and the filtrate was subjected to UV-visible spectral and HPLC analyses. The results confirmed that CDNS did not contain phenol. The pure CDNS was then dried in an oven at 90 °C for 12 h.

2.3 | Synthesis of Amine-Functionalized CDNS (CDNS-N)

A solution of AEAPTMS (4 ml in 20 ml of dry toluene) was added to a suspension of CDNS (1.2 g) in dry toluene (40 ml). The mixture was then subjected to ultrasonic irradiation at a power of 100 W for 30 min. Subsequently, the obtained suspension was refluxed for 24 h. Upon completion of the process, the white solid (2) was filtered and washed repeatedly with dry toluene and dried at 80 °C overnight.

2.4 | Synthesis of Cl-Functionalized Sepiolite (Sepiolite-Cl)

Sepiolite (1 g) was suspended in xylene (100 ml) and mixed vigorously for 15 min. Subsequently, 3-chloropropyltrimethoxysilane (2.5 ml) was added dropwise to the solution. The resulting suspension was then stirred for 24 h. Sepiolite-Cl was obtained by drying in a vacuum oven at 90 °C overnight.

2.5 | Synthesis of CDNS–Sepiolite Hybrid

To a mixture of sepiolite-Cl (2.25 g) in dry toluene (100 ml), ammonia (0.5 ml) as a catalyst was added. Subsequently, CDNS-N (0.75 g) was crushed and well dispersed under ultrasonic irradiation of 100 W in toluene and then added to the aforementioned mixture. Subsequently, the suspension was refluxed for 24 h. Upon completion of the reaction, the solid was filtered and poured in water. Then the aqueous suspension was centrifuged. Sepiolite–CDNS that was at the top of the centrifuged mixture was gathered, washed with toluene repeatedly and dried in a vacuum oven at 100 °C. The conjugation of sepiolite and CDNS was achieved through routine

nucleophilic substitution reaction of sepiolite-Cl and CDNS-N. More precisely, the electron pair of amine on CDNS-N attacked the Cl-sepiolite and substituted Cl (Cl acted as an active leaving group).

2.6 | Immobilization of Pd Nanoparticles on CDNS–sepiolite

CDNS–sepiolite (1.2 g) was suspended in dry toluene (20 ml) and stirred vigorously for 15 min. Then, a solution of Pd (OAc)₂ (0.02 g) in MeOH (12 ml) was slowly added. The obtained suspension was then stirred at ambient temperature for 10 h. To obtain Pd(0) nanoparticles, NaBH₄ was used as reducing agent. More precisely, NaBH₄ was dissolved in a mixture of toluene and MeOH (10 ml, 0.2 N) and introduced to the abovementioned suspension. Then, the suspension was stirred for 4 h. Finally, Pd@CDNS-sepiolite was obtained (70% yield) by washing with MeOH and drying in an oven at 60 °C for 12 h (Figure 1).

To prepare Pd@sepiolite and Pd@CDNS, similar methodologies were used, except that sepiolite and CDNS-N were used, respectively, for immobilization of Pd nanoparticles.

2.7 | Typical Procedure for Sonogashira Reaction

To a mixture of the organic reagents, i.e. aryl halide (1.0 mmol) and acetylene (1.2 mmol) in EtOH (20 ml), Pd@CDNS-sepiolite (25 mg) and K₂CO₃ (2.0 mmol) were added. Then, the resulting mixture was heated at 50 °C with stirring. HPLC was used for monitoring the progress of the reaction. Upon completion of the reaction, the catalyst was filtered off and the reaction mixture was cooled to room temperature. Then, the organic layer was extracted with diethyl ether and purified by column chromatography over silica gel using hexane–ethyl acetate (4:1) as eluent.

2.8 | Typical Procedure for Catalytic Mizoroki–Heck Reaction

To a mixture of aryl halide (1.0 mmol) and alkene (1.5 mmol) in EtOH (20 ml), K₂CO₃ (2 mmol) and Pd@CDNS-sepiolite (30 mg) were added and the resulting mixture was stirred at 100 °C for the appropriate reaction time. Upon completion of the reaction, Pd@CDNS-sepiolite was filtered, washed with EtOH and dried at 70 °C for further use. The organic layer, extracted with diethyl ether, was washed with water, separated and dried over anhydrous Na₂SO₄. Recrystallization was used for further purification.

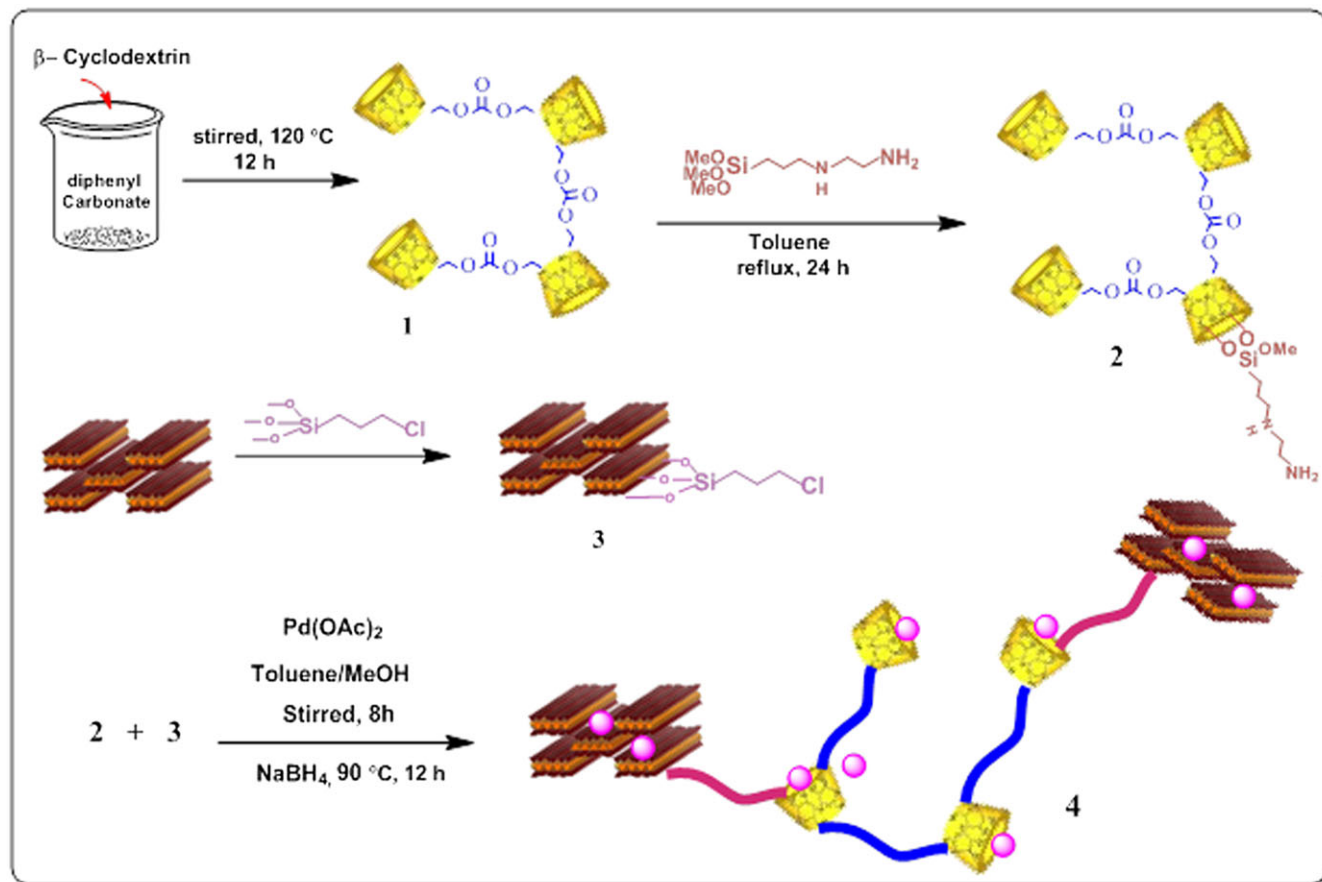


FIGURE 1 Synthetic procedure for preparation of Pd@CDNS-sepiolite

3 | RESULTS AND DISCUSSION

3.1 | Catalyst Characterization

In Figure 2 the FT-IR spectra of CDNS, CDNS-N, sepiolite, sepiolite-Cl, CDNS-sepiolite and Pd@CDNS-sepiolite are depicted. The FT-IR spectrum of sepiolite exhibits characteristic bands at 3561, 3453 and 645 cm^{-1} , which can be assigned to the stretching and bending vibrations of —OH groups. These functional groups are attached to octahedral Mg ions located in the interior blocks of sepiolite.^[52] The observed band at 1016 cm^{-1} is representative of Si—O stretching. The FT-IR spectrum of sepiolite-Cl is very similar to that of pristine sepiolite. This observation is not beyond expectation, as the content of organosilane is very low (estimated to be about 5 wt% via TGA, discussed below). The FT-IR spectrum of CDNS showed a characteristic band at 3350 cm^{-1} that is due to the —OH functional group. The band at 2923 cm^{-1} can be assigned to the —CH_2 functional groups. Moreover, the band at 1775 cm^{-1} in the spectrum of CDNS-N can be attributed to the C=O functional group. Comparing the FT-IR spectrum of CDNS with that of CDNS-N, it can be seen that both spectra are similar and only a small

shift is observed for the CDNS-N spectrum. Again, the similarity of these two spectra can be attributed to the low amount of organosilane on CDNS. The FT-IR spectra of CDNS-sepiolite and Pd@CDNS-sepiolite are also depicted in Figure 2. The characteristic bands of CDNS-N and sepiolite are present in these spectra. This observation can confirm the formation of CDNS-sepiolite.

The XRD patterns of sepiolite and Pd@CDNS-sepiolite are illustrated in Figure 3. According to the literature,^[20] the reflection bands observed at $2\theta = 7.6^\circ$, 19.6° , 20.70° , 23.9° , 28° , 27.38° , 34.4° , 37.54° and 40.1° can be attributed to the sepiolite structure.^[20] Other observed peaks can be attributed to the impurities of sepiolite. As depicted, the characteristic peaks of Pd(0) nanoparticles cannot be detected as the Pd characteristic peaks are generally small and the amount of Pd nanoparticles is very low, as confirmed by ICP analysis (discussed below). Considering the literature, a high distribution of Pd nanoparticles can also justify the fact that the characteristic peaks of Pd nanoparticles were not observed.^[53]

The SEM images of CDNS, CDNS-N, sepiolite, CDNS-sepiolite and Pd@CDNS-sepiolite are depicted in Figure 4. As shown, CDNS exhibited aggregate-like morphology. Upon functionalization with organosilanes, the

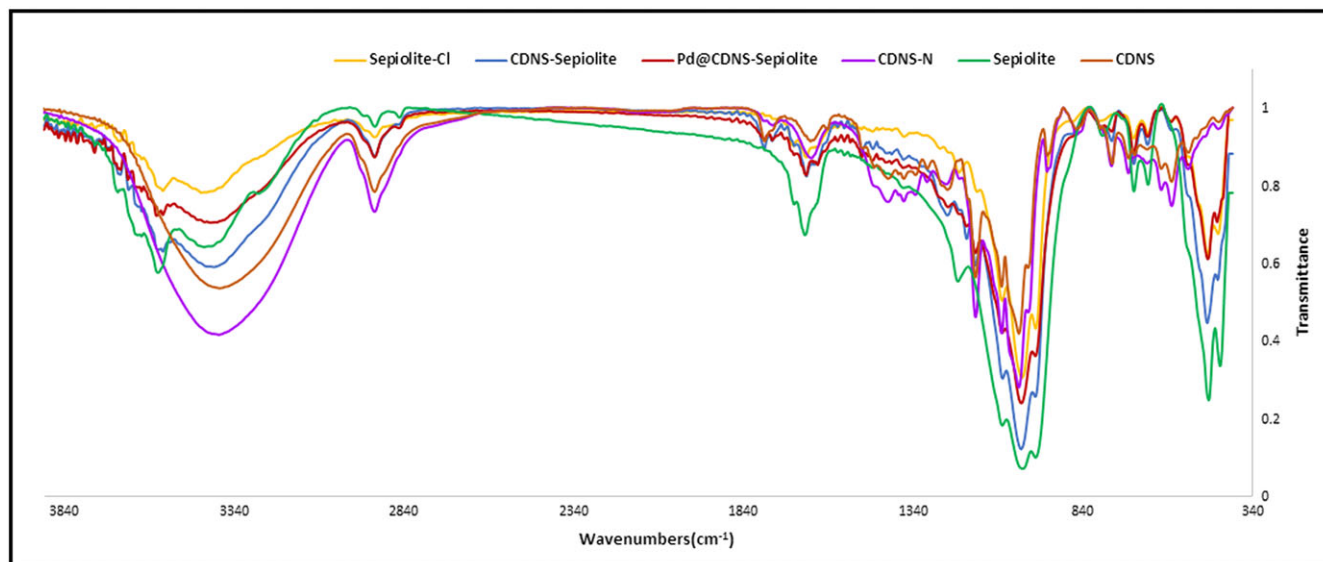


FIGURE 2 FT-IR spectra of CDNS, sepiolite, CDNS-N, sepiolite-Cl, CDNS-sepiolite and Pd@CDNS-sepiolite

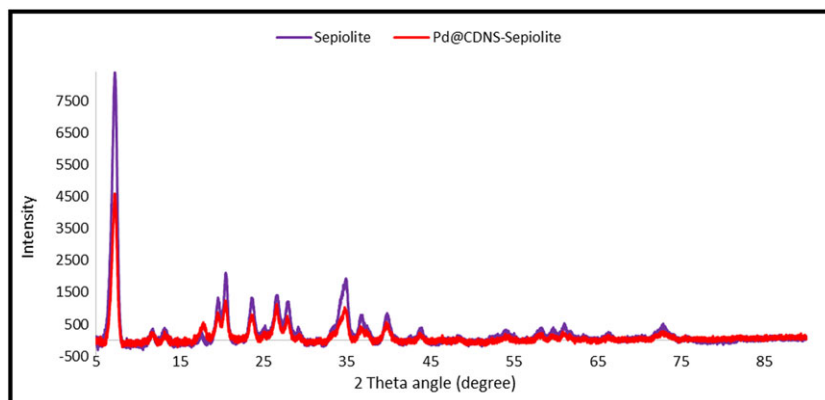


FIGURE 3 XRD patterns of Pd@CDNS-sepiolite and sepiolite

morphology of CDNS changed to some extent. However, CDNS-N still showed aggregate-like morphology. The SEM image of sepiolite is in good accordance with the literature^[52] and exhibited needle-like morphology. As shown, upon conjugation with CDNS, sepiolite preserved its needle-like morphology. Incorporation of Pd nanoparticles also did not alter markedly the needle-like morphology. However, some small aggregates can be detected in the SEM images of Pd@CDNS-sepiolite.

The EDS spectrum of Pd@CDNS-sepiolite (Figure 4) showed Si, O and Mg atoms, which are mainly representative of sepiolite. Moreover, the presence of Pd atoms can confirm the incorporation of Pd(0) nanoparticles in the hybrid catalyst. Also, the observation of C and N atoms can be attributed to the presence of CDNS-N. However, EDS analysis cannot solely confirm the formation of CDNS-N. Hence, the formation of CDNS and the final catalyst was further confirmed using other techniques (discussed below).

In Figure 5, TEM images of sepiolite and Pd@CDNS-sepiolite are depicted. As shown, the TEM image of pristine sepiolite exhibited needle-like morphology, which is in good agreement with previous reports.^[54,55] A comparison of the TEM images of the catalyst and that of pristine sepiolite showed that the catalyst is slightly different from the sepiolite and exhibited a slightly more compact morphology. In the TEM images of Pd@CDNS-sepiolite, it can be seen that the sepiolite needles are covered with CDNS to some extent. This surface functionalization resulted in the slightly aggregated morphology. Considering the TEM images, in which the Pd nanoparticles are not detectable, it can be concluded that Pd nanoparticles can locate within the interlayer of sepiolite. Moreover, according to the literature, Pd can also be accommodated within the cavities of CDs.^[56] Hence, another possibility for accommodation of Pd nanoparticles is the cavities of CDs in CDNS.

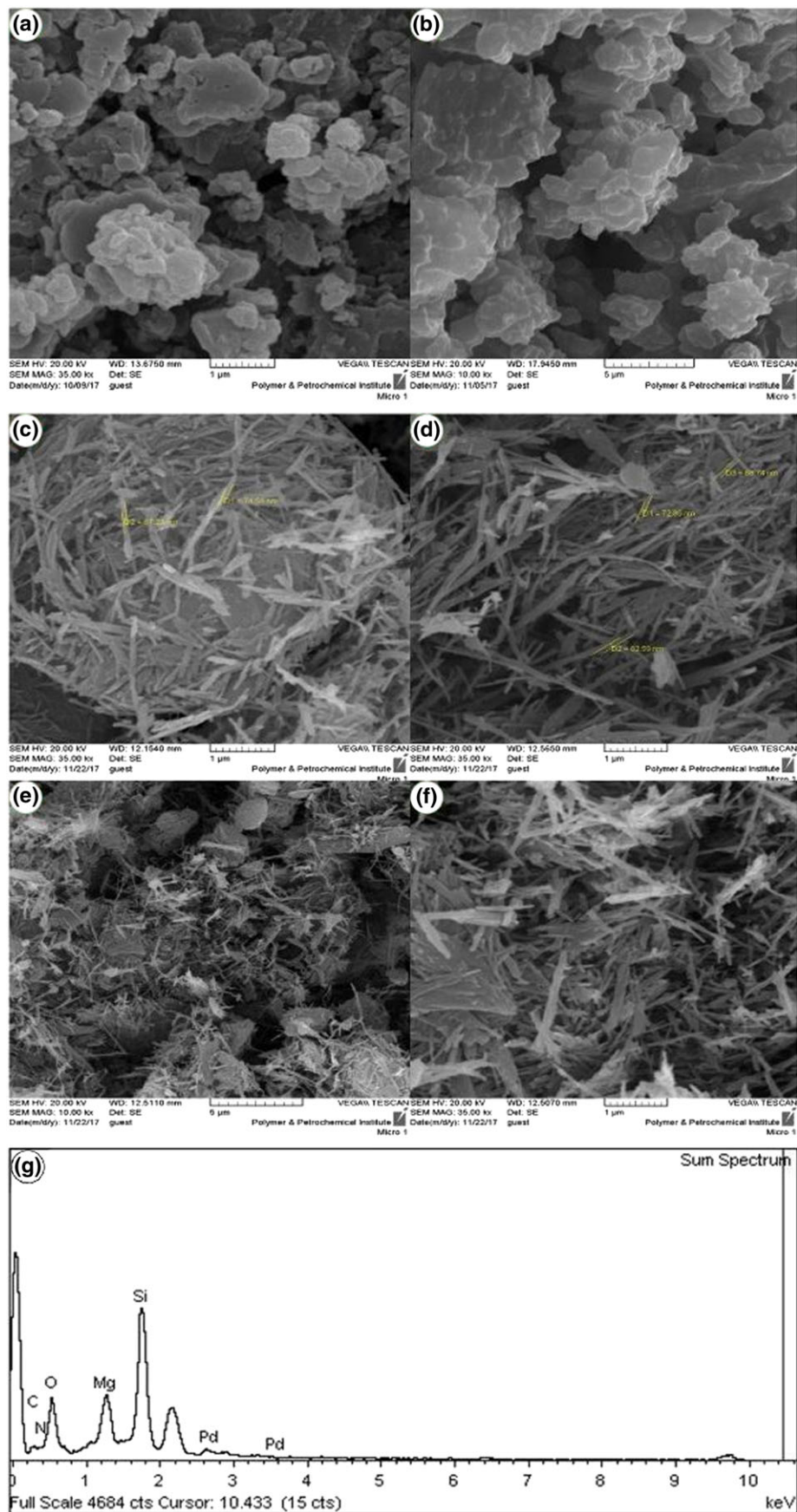


FIGURE 4 SEM images of (a) CDNS, (b) CDNS-N, (c) sepiolite, (d) CDNS-sepiolite and (e, f) Pd@CDNS-sepiolite. (g) EDS analysis of Pd@CDNS-sepiolite

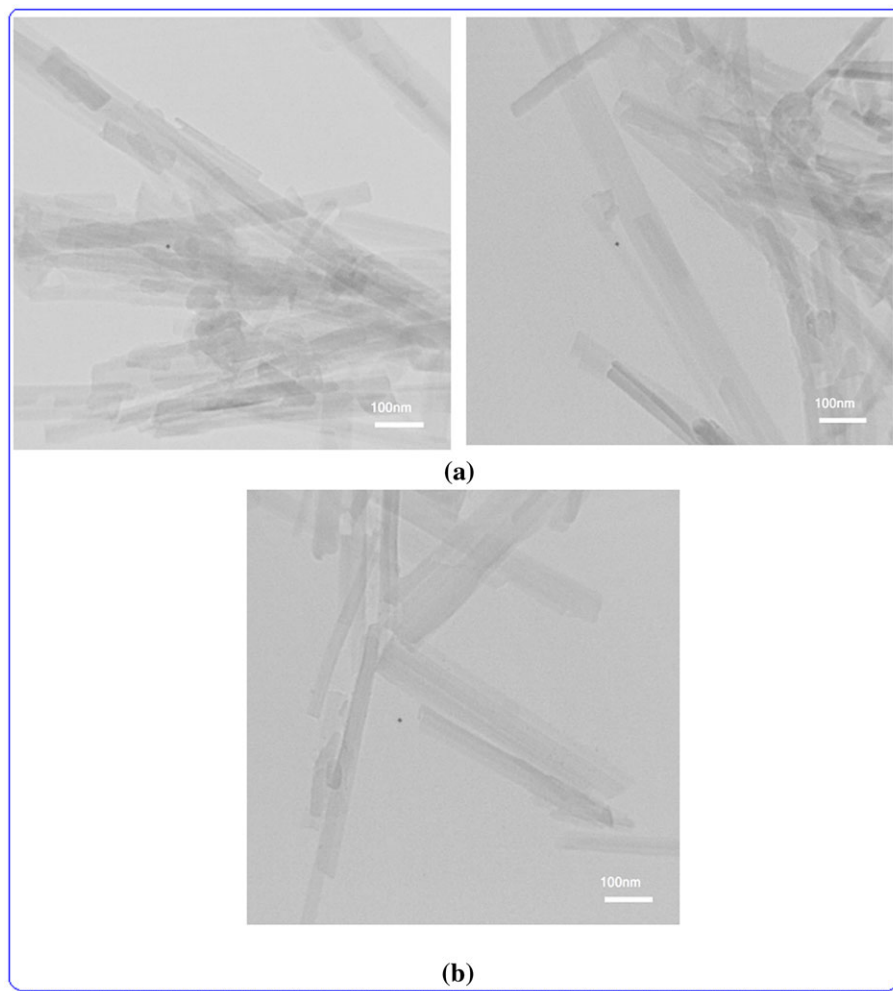


FIGURE 5 TEM images of (a) Pd@CDNS-sepiolite and (b) sepiolite

ICP-AES analysis was applied to calculate the content of Pd nanoparticles in Pd@CDNS-sepiolite. To prepare a sample for analysis, a known amount of Pd@CDNS-sepiolite (0.002 g) was digested in a concentrated 1:5 mixture (18 ml) of acidic solution of HNO_3 and HCl (6 M) and then the obtained extract was analysed using ICP-AES. Using this methodology and knowing the starting amount of the catalyst, the content of Pd nanoparticles was estimated to be about 0.5 wt%.

In Figure 6, the nitrogen adsorption–desorption isotherm of Pd@CDNS-sepiolite is depicted. As illustrated, the obtained isotherm is of type II with H3 hysteresis loops.^[57] This observation can imply that Pd@CDNS-sepiolite is of a porous nature. It is worth mentioning that the nitrogen adsorption–desorption isotherm of Pd@CDNS-sepiolite is distinguished from that of CDNS (Figure S2 in supporting information).

The specific surface area of Pd@CDNS-sepiolite was calculated to be $130 \text{ m}^2 \text{ g}^{-1}$, which was lower than that

of sepiolite ($161 \text{ m}^2 \text{ g}^{-1}$) and higher than that of CDNS (*ca* $10 \text{ m}^2 \text{ g}^{-1}$).

The catalyst was also investigated using TGA (Figure 7). To estimate the content of organic functionalities, the thermograms of sepiolite-Cl and CDNS-sepiolite were also recorded (Figure 7). Sepiolite-Cl exhibited two weight losses: the first one at about $120 \text{ }^\circ\text{C}$ can be assigned to the loss of water and the second at about $330 \text{ }^\circ\text{C}$ is due to loss of organosilane. Using this thermogram, the content of organosilane on the sepiolite was estimated to be about 5 wt%.

The thermogram of CDNS-sepiolite showed three weight losses. The first was at about $110 \text{ }^\circ\text{C}$, which can be due to loss of water, the others at about 320 and $560 \text{ }^\circ\text{C}$. These weight losses can be due to the degradation of CDNS-N.^[50] Using this analysis, the content of CDNS-N was calculated to be about 15 wt%.

Considering the above discussion, the weight losses in the thermogram of the catalyst can be attributed to the

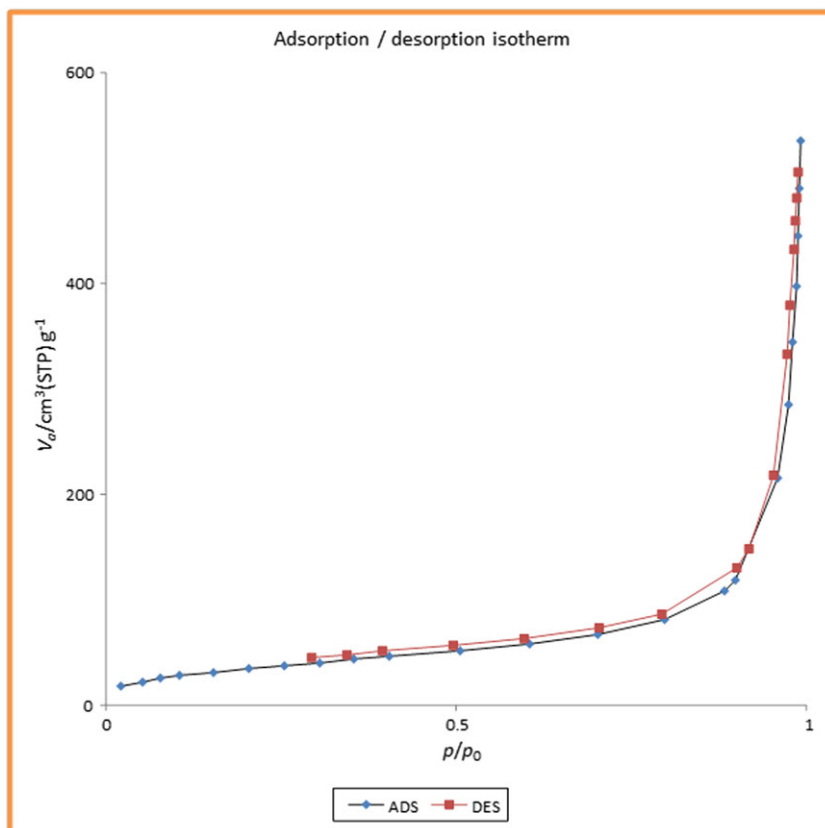


FIGURE 6 Nitrogen adsorption-desorption isotherms of Pd@CDNS-sepiolite

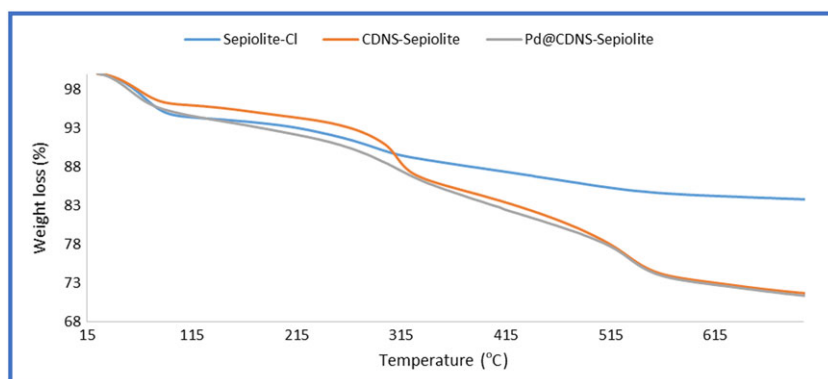


FIGURE 7 TGA curves of Pd@CDNS-sepiolite, sepiolite-Cl and CDNS-sepiolite

loss of water (about 150 °C) and degradation of CDNS and organosilanes (about 320 and 530 °C).

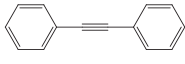
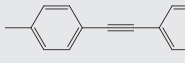
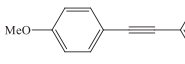
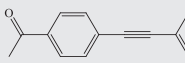
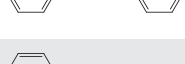
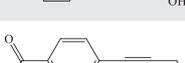
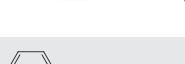
3.2 | Catalytic Activity

After verifying the structure of Pd@CDNS-sepiolite, the study of its catalytic activity was undertaken. In this line, the utility of Pd@CDNS-sepiolite for promoting C–C coupling reactions, Heck and Sonogashira reactions, was investigated. Initially, two model reactions were selected to study the effects of reaction variables and to optimize the reaction conditions.

For the Sonogashira reaction, the reaction of iodobenzene with acetylene was selected as a model,

while the reaction of methyl acrylate and iodobenzene was chosen for the Heck reaction. First, the model reactions were performed in the presence of cost-effective K_2CO_3 as base and water as solvent at room temperature. The results established that, although the reactions proceeded in the absence of copper and ligand, the yields of the products were moderate (Tables S1 and S2 in supporting information). Hence, to improve the yield of the desired products, the reactions were performed in various solvents, such as CH_3CN , toluene and $CHCl_3$ (Tables S1 and S2 in supporting information). Gratifyingly, use of EtOH as solvent markedly increased the yield of the reaction. To further improve the yield of the products, the reaction was examined at elevated

TABLE 1 Sonogashira reaction of aryl halides with alkynes^a

Entry	Aryl halide	Terminal alkyne	Product	Time (h:min)	Yield (%) ^b
1				1:45	94
2				3:30	88
3				3:00	93
4				2:00	92
5				3:30	80
6				3:30	70
7				3:50	66
8				3:20	73
9				4:40	60
10				3:30	93
11				3:00	90
12				3:30	92
13				4:30	90
14				4:30	85
15				4:30	93
16				5:15	80

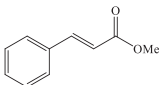
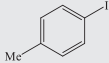
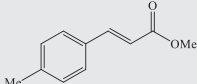
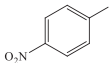
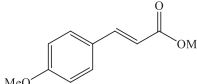
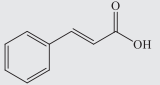
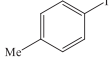
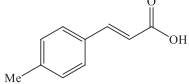
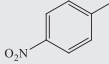
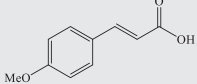
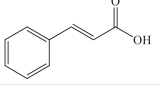
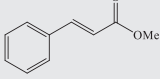
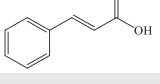
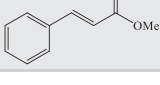
^aReactions were run with 1 mmol of aryl halide, 1.2 mmol of acetylene and 2 mmol of K_2CO_3 in the presence of the catalyst in EtOH.

^bIsolated yield.

temperatures (50 and 70 °C; Tables S1 and S2 in supporting information). It was found that an increase of the temperature to an optimum amount (50 °C for Sonogashira reaction and 70 °C for Heck reaction) increased the yields of the products. However, further

increase of the temperature had a detrimental effect and decreased the yields of the reactions. The effect of base was also investigated using various bases, such as NaOH, CS_2CO_3 and KOH (Tables S1 and S2 in supporting information). It was found that K_2CO_3 was

TABLE 2 Heck reaction of aryl halides with alkenes^a

Entry	Aryl halide	Alkene	Product	Time (h)	Yield (%) ^b
1				3	86
2				2	90
3				2	80
4				2.5	90
5				2	90
6				2	92
7				3	85
8				3	88
9				4.2	70
10				4	73

^aReaction conditions: aryl halide (1.0 mmol) and alkene (1.5 mmol) in EtOH (20 ml) in the presence of K₂CO₃ (2 mmol) and catalyst.

^bIsolated yield.

the best base for these protocols. Moreover, optimization of the amount of the base was performed and the optimum amount of K₂CO₃ was estimated to be 2 mmol. Finally, the optimum amount of catalyst was determined using various amounts of Pd@CDNS-sepiolite (0.01–0.03 mg; Tables S1 and S2 in supporting information). It was found that using 0.02 g catalyst led to the highest yields of the products.

Next, to elucidate whether these protocols could be generalized, various Heck and Sonogashira products were synthesized using a selection of alkenes, alkynes and aryl halides with a variety of electronic and steric properties (Tables 1 and 2). All employed reagents could undergo the corresponding coupling reactions and resulted in products in good to high yields. Of note, use of aryl iodides led to higher yields compared to aryl chlorides and aryl bromides. Furthermore,

reagents with less steric hindrance resulted in higher yields.

To study the effect of hybridization of CDNS and sepiolite, two control catalysts, Pd@CDNS and Pd@sepiolite, were prepared (Section 2) and then their Pd content was estimated via ICP and compared with that of Pd@CDNS-sepiolite. The results confirmed that the content of Pd in Pd@CDNS-sepiolite was higher than that in Pd@CDNS and Pd@sepiolite, indicating that hybridizing CDNS and sepiolite can improve the anchoring of Pd species. Notably, due to the higher content of Pd in Pd@CDNS-sepiolite, it was more efficient compared to Pd@sepiolite and Pd@CDNS.

According to the literature, the main catalytic active species for the coupling reactions is Pd.^[58] The proposed mechanism for the ligand- and copper-free Sonogashira coupling reaction in the presence of the catalyst is as follows.

First, the reaction is commenced by activation of terminal C—H of alkyne by the catalyst. Subsequently, deprotonation by K_2CO_3 and formation of an intermediate, potassium acetylide, occur (Figure 8). Aryl halide is activated by Pd@CDNS-sepiolite to afford another intermediate, $ArPdX$, that undergoes halide displacement to form arylpalladium acetylide. C—C coupling product as well as Pd@CDNS-sepiolite are produced by reductive elimination.

3.3 | Catalyst Recyclability

In the last part of the investigation, the recyclability of Pd@CDNS-sepiolite was studied. In this line, after the end of Sonogashira model reaction, the catalyst was filtered, washed and dried (Section 2) and subjected to the next run of the model reaction. This cycle was repeated for five consecutive reaction runs. A comparison of the yields of the product in the case of fresh and recycled catalyst established that Pd@CDNS-sepiolite could be successfully recycled with slight loss of catalytic activity (Figure 9).

To further investigate the effect of recycling, ICP-AES analysis was used to investigate the leaching of Pd upon recycling. Low leaching of Pd was observed in the case of the catalyst recycled for the fifth time. This can justify the observed decrease in the yield of the products upon catalyst reuse.

Next, the stability of Pd@CDNS-sepiolite upon recycling was investigated by comparing the FT-IR spectra of fresh and recycled Pd@CDNS-sepiolite. As shown in Figure 10, the spectra of fresh and recycled catalyst are very similar, implying that the structure of Pd@CDNS-sepiolite was preserved upon recycling. It is worth noting that recycling of the catalyst may result in partial hydrolysis of CDNS. Hence, the observed decrease of the yield of the model reaction can be attributed to both Pd leaching and hydrolysis of CDNS.

The morphology of the recycled Pd@CDNS-sepiolite was also studied by recording the SEM image of the recycled catalyst. As shown in Figure 11, the morphology

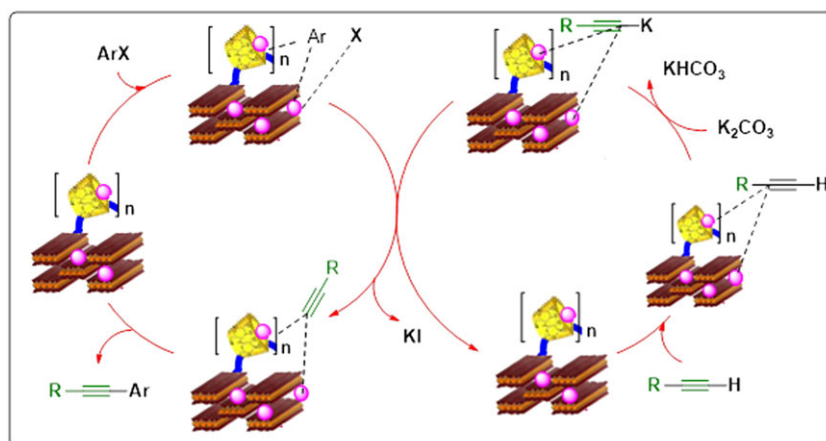


FIGURE 8 Plausible mechanism for promotion of Sonogashira coupling reaction

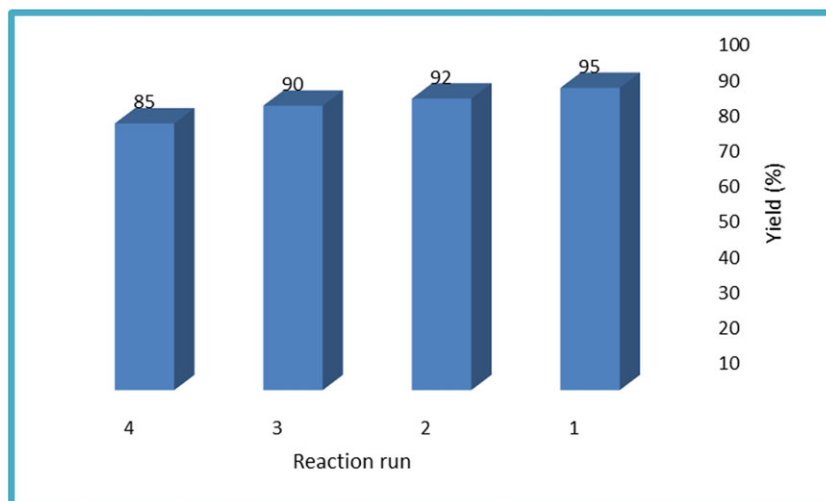


FIGURE 9 Efficiency of catalyst for promoting model reaction after several reaction runs

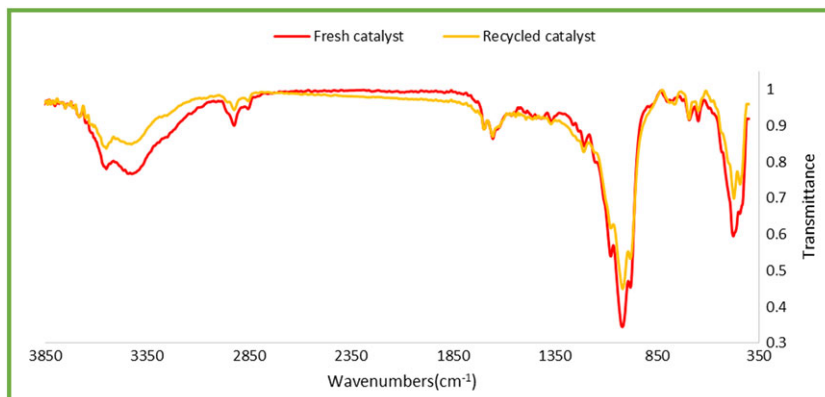


FIGURE 10 FT-IR spectra of fresh and recycled Pd@CDNS-sepiolite

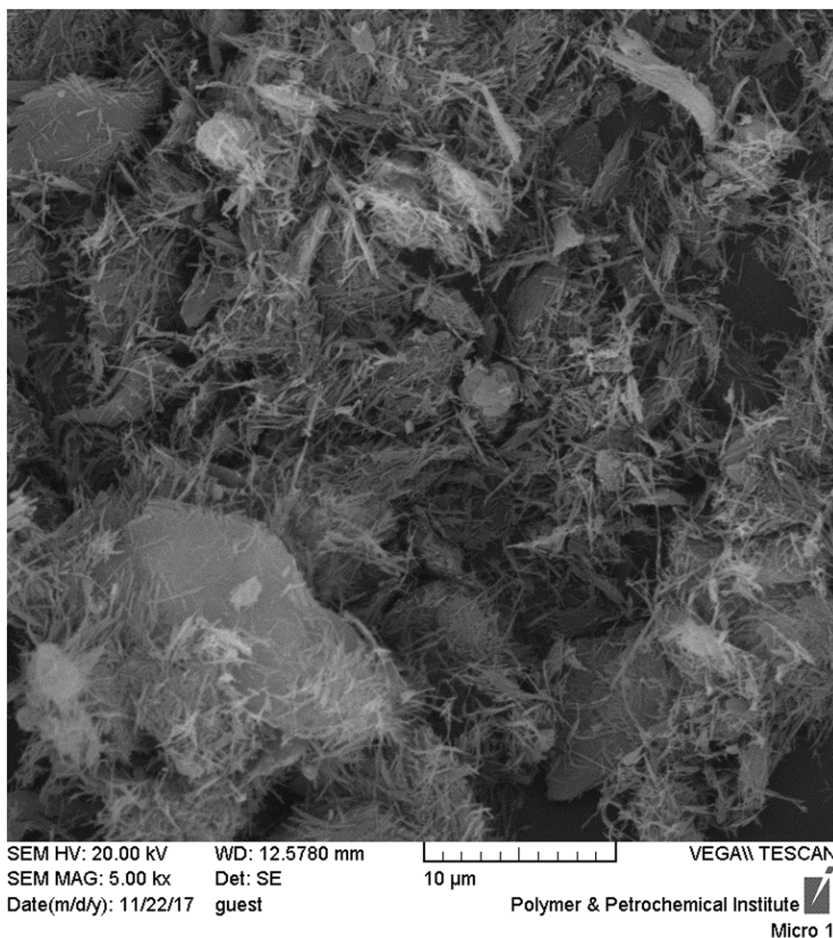


FIGURE 11 SEM image of recycled catalyst.

of the recycled catalyst is slightly more aggregated but still very similar to that of fresh catalyst, implying that recycling did not markedly affect the morphology.

4 | CONCLUSIONS

CDNS-N reacted with sepiolite-Cl to afford CDNS-sepiolite which subsequently served as an efficient support for

immobilization of Pd nanoparticles. The catalytic activity of Pd@CDNS-sepiolite for ligand- and copper-free Sonogashira and Heck coupling reactions was confirmed. Moreover, it was proved that the catalyst was recyclable and could be easily recovered and recycled for several consecutive reaction runs with only slight loss of the catalytic activity and slight leaching of Pd(0) nanoparticles.

ACKNOWLEDGEMENTS

The authors are grateful for partial financial support from Iran Polymer and Petrochemical Institute and Alzahra University. MMH is also grateful to Iran National Science Foundation for an individual grant. The contribution of Professor Atai is gratefully appreciated for providing sepiolite clay.

ORCID

Samah Sadjadi  <http://orcid.org/0000-0002-6884-4328>

Majid M. Heravi  <http://orcid.org/0000-0003-2978-1157>

REFERENCES

- [1] F. Trotta, in *Cyclodextrins in Pharmaceutics, Cosmetics, and Biomedicine: Current and Future Industrial Applications*, (Ed: E. Bilenjoy), John Wiley, Hoboken, NJ **2011** 323.
- [2] G. Tejashri, B. Amrita, J. Darshana, *Acta Pharm.* **2013**, *63*, 335.
- [3] F. Trotta, R. Cavalli, W. Tumiatti, O. Zerbinati, C. Roggero, R. Vallerio, Ultrasound-assisted synthesis of cyclodextrin-based nanosponges, WO Patent, **2006**, WO2006002814A1.
- [4] F. Trotta, R. Cavalli, K. Martina, M. Biasizzo, J. Vitillo, S. Bordiga, P. Vavia, K. Ansari, *J. Inclusion Phenom. Macroscopic Chem.* **2011**, *71*, 189.
- [5] S. Swaminathan, L. Pastero, L. Serpe, F. Trotta, P. Vavia, D. Aquilano, M. Trotta, G. P. Zara, R. Cavalli, *Eur. J. Pharm. Biopharm.* **2010**, *74*, 193.
- [6] M. Shringirishi, S. K. Prajapati, A. Mahor, S. Alok, P. Yadav, A. Verma, *Asian Pac. J. Trop. Dis.* **2014**, *4*, S519.
- [7] S. Torne, S. Darandale, P. Vavia, F. Trotta, R. Cavalli, *Pharm. Dev. Technol.* **2013**, *18*, 619.
- [8] P. Shende, K. Deshmukh, F. Trotta, F. Caldera, *Int. J. Pharm.* **2013**, *456*, 95.
- [9] R. Cavalli, F. Trotta, W. Tumiatti, *J. Incl. Phenom.* **2006**, *56*, 209.
- [10] S. Anandam, S. Selvamuthukumar, *J. Mater. Sci.* **2014**, *49*, 8140.
- [11] S. Swaminathan, R. Cavalli, F. Trotta, *WIREs Nanomed. Nanobiotechnol.* **2016**, *8*, 579.
- [12] F. Trotta, C. Dianzani, F. Caldera, B. Moggetti, R. Cavalli, *Expert Opin. Drug Deliv.* **2014**, *11*, 931.
- [13] F. Caldera, M. Tannous, R. Cavalli, M. Zanetti, F. Trotta, *Int. J. Pharm.* **2017**, *531*, 470.
- [14] G. Di Nardo, C. Roggero, S. Campolongo, F. Valetti, F. Trotta, G. Gilardi, *Dalton Trans.* **2009**, 6507.
- [15] B. Boscolo, F. Trotta, E. Ghibaudi, *J. Mol. Catal. B* **2010**, *22*, 155.
- [16] G. Cravotto, E. C. Calcio Gaudino, S. Tagliapietra, D. Carnaroglio, A. Procopio, *Green Process Synth.* **2012**, *1*, 269.
- [17] P. Cintas, G. Cravotto, E. C. Gaudino, L. Orio, L. Boffa, *Cat. Sci. Technol.* **2012**, *2*, 85.
- [18] M. Arkas, R. Allabashi, D. Tsiourvas, E.-M. Mattausch, R. Perfle, *Environ. Sci. Technol.* **2006**, *40*, 2771.
- [19] Y. Lv, F. Hao, P. Liu, S. Xiong, H. Luo, *J. Mol. Catal. A* **2017**, *426*, 15.
- [20] N. Degirmenbasi, N. Boz, D. M. Kalyon, *Appl Catal B* **2014**, *150*, 147.
- [21] L. Guishui, C. Lijun, Z. Bing, L. Yi, *Mater. Lett.* **2016**, *168*, 143.
- [22] S. Liu, D. Zhu, J. Zhu, Q. Yang, H. Wu, *J. Environ. Sci.* **2017**, *60*, 43.
- [23] F. Zhou, C. Yan, H. Wang, S. Zhou, S. Komarneni, *Appl. Clay Sci.* **2017**, *146*, 246.
- [24] Y. Ma, X. Wu, G. Zhang, *Appl Catal B* **2017**, *205*, 262.
- [25] B.-N. Lin, S.-H. Huang, W.-Y. Wu, C.-Y. Mou, F.-Y. Tsai, *Molecules* **2010**, *15*, 9157.
- [26] A. R. Hajipour, Z. Shirdashtzade, G. Azizi, *Appl. Organomet. Chem.* **2014**, *28*, 696.
- [27] R. Chinchilla, C. Nájera, *Chem. Soc. Rev.* **2011**, *40*, 5084.
- [28] S. N. Jadhav, A. S. Kumbhar, C. V. Rode, R. S. Salunkhe, *Green Chem.* **2016**, *18*, 1898.
- [29] A. R. Gholap, K. Venkatesan, R. Pasricha, T. Daniel, R. J. Lahoti, K. V. Srinivasan, *J. Org. Chem.* **2005**, *70*, 4869.
- [30] R. Thorwirth, A. Stolle, B. Ondruschka, *Green Chem.* **2010**, *12*, 985.
- [31] M. Nasrollahzadeh, M. Maham, M. M. Tohidi, *J. Mol. Catal. A* **2014**, *391*, 83.
- [32] M. Bakherad, *Appl. Organomet. Chem.* **2013**, *27*, 125.
- [33] M. Bakherad, R. Doosti, M. Mirzaee, K. Jadidi, *Tetrahedron* **2017**, *73*, 3281.
- [34] P. V. Rathod, V. H. Jadhav, *Tetrahedron Lett.* **2017**, *58*, 1006.
- [35] M. Esmaeilpour, A. Sardarian, J. Javidi, *Cat. Sci. Technol.* **2016**, *6*, 4005.
- [36] M. Nasrollahzadeh, S. M. Sajadi, M. Maham, A. Ehsani, *RSC Adv.* **2015**, *5*, 2562.
- [37] R. Zhou, W. Wang, Z.-J. Jiang, H.-Y. Fu, X.-L. Zheng, C.-C. Zhang, H. Chen, R.-X. Li, *Cat. Sci. Technol.* **2014**, *4*, 746.
- [38] M. Nasrollahzadeh, M. Khalaj, A. Ehsani, *Tetrahedron Lett.* **2014**, *55*, 5298.
- [39] M. Shunmughanathan, P. Puthiaraj, K. Pitchumani, *ChemCatChem* **2015**, *7*, 666.
- [40] A. S. Roy, J. Mondal, B. Banerjee, P. Mondal, A. Bhaumik, S. Manirul Islam, *Appl. Catal. A* **2014**, *469*, 320.
- [41] A. Kumbhar, S. Jadhav, S. Kamble, G. Rashinkar, R. Salunkhe, *Tetrahedron Lett.* **2013**, *54*, 1331.
- [42] S. Wu, H. Ma, X. Jia, Y. Zhong, Z. Lei, *Tetrahedron* **2011**, *67*, 250.
- [43] S.-S. Yi, D.-H. Lee, E. Sin, Y.-S. Lee, *Tetrahedron Lett.* **2007**, *48*, 6771.
- [44] E. Sin, S.-S. Yi, Y.-S. Lee, *J. Mol. Catal. A* **2010**, *315*, 99.
- [45] H. Veisi, M. Ghadermazi, A. Naderi, *Appl. Organomet. Chem.* **2016**, *30*, 341.
- [46] S. Sadjadi, T. Hosseinnejad, M. Malmir, M. M. Heravi, *New J. Chem.* **2017**, *41*, 13935.
- [47] S. Sadjadi, M. M. Heravi, *RSC Adv.* **2016**, *6*, 88588.
- [48] S. Sadjadi, M. M. Heravi, M. Daraie, *Res. Chem. Intermed.* **2017**, *43*, 2201.
- [49] S. Sadjad, M. Atai, *Appl. Clay Sci.* **2018**, *153*, 78.

- [50] S. Sadjadi, M. M. Heravi, M. Daraie, *J. Mol. Liq.* **2017**, *231*, 98.
- [51] R. Yang, Y. Wang, M. Li, Y. Hong, *ACS Sustain. Chem. Eng.* **2014**, *2*, 1270.
- [52] R. Liu, J. Wang, J. Zhang, S. Xie, X. Wang, Z. Ji, *Micropor. Mesopor. Mater.* **2017**, *248*, 234.
- [53] S. Mallik, S. S. Dash, K. M. Parida, B. K. Mohapatra, *J. Colloid Interface Sci.* **2006**, *300*, 237.
- [54] T. H. Liu, X. J. Chen, Y. Z. Dai, L. L. Zhou, J. Guo, S. S. Ai, *J. Alloys Compd.* **2015**, *649*, 244.
- [55] K. Núñez, R. Gallego, J. M. Pastor, J. C. Merinoa, *Appl. Clay Sci.* **2014**, *101*, 73.
- [56] B. Kaboudin, H. Salemi, R. Mostafalu, F. Kazemi, T. Yokomatsu, *J. Organomet. Chem.* **2016**, *818*, 195.
- [57] P. Yuan, P. D. Southon, Z. Liu, M. E. R. Green, J. M. Hook, S. J. Antill, C. J. Kepert, *J. Phys. Chem. C* **2008**, *112*, 15742.
- [58] A. S. Camacho, I. Martin-Garcia, C. Contreras-Celedon, L. Chacon-Garcia, F. Alonso, *Cat. Sci. Technol.* **2017**, *7*, 2262.

SUPPORTING INFORMATION

Additional supporting information may be found online in the Supporting Information section at the end of the article.

How to cite this article: Sadjadi S, Heravi MM, Raja M, Kahangi FG. Palladium nanoparticles immobilized on sepiolite–cyclodextrin nanosponge hybrid: Efficient heterogeneous catalyst for ligand- and copper-free C–C coupling reactions. *Appl Organometal Chem.* 2018;e4508. <https://doi.org/10.1002/aoc.4508>